



## Near Real-Time Estimation of Spatial Distribution for Ground Motion Parameters During Recent Earthquakes in Japan

Khosrow T. Shabestari<sup>1</sup>, Fumio Yamazaki<sup>2</sup>, and Jun Saita<sup>3</sup>

<sup>1</sup> Research Scientist, Earthquake Disaster Mitigation Research Center, NIED  
2465-1, Mikiyama, Miki, Hyogo 673-0433, Japan  
khosrow@edm.bosai.go.jp

<sup>2</sup> Professor, Institute of Industrial Science, University of Tokyo  
4-6-1 Komaba, Meguro-ku, Tokyo 153-8505, Japan

<sup>3</sup> Research Engineer, System and Data Research, SDR Company  
3-25-3 Fujimi-dai, Kunitachi-shi, Tokyo 186-0003, Japan

### ABSTARCT

Estimation of spatial distribution for the earthquake ground motion indices plays an important role in early-stage damage assessments for rescue operations by disaster management agencies as well as for damage studies of urban structures. However, subsurface geology layers and local soil conditions lead on soil amplification that may be susceptible to distribution of estimated ground motion parameters on the surface. In this case study the applicability of the nationwide proposed GIS-based soil amplification ratios by Yamazaki et al. (2000) in the October 6, 2000 Tottori-ken Seibu (western Tottori Prefecture) and the March 24, 2001 Geiyo earthquakes in Japan have been examined. First, the ground motion parameters were converted to those at the hypothetical ground base-rock level (outcrop) using the amplification ratio for each 1 km x 1 km mesh size of geomorphological and subsurface geology classification unit. Then a Kriging method with the attenuation relationship at the base-rock as a trend component is applied. Finally the distribution of spatial ground motion parameters on the ground surface are obtained by multiplying those values with the GIS-based amplification factors for the entire region.

### 1. INTRODUCTION

Recent damaging earthquakes in urban areas emphasize the importance of early damage assessment in earthquake disaster mitigation<sup>2,3</sup>. Magnitude and depth information alone following a large magnitude earthquake cannot represent the complex damage pattern. More detailed information, including data obtained from a nationwide or a dense strong-ground-motion network, is required for decision-making by emergency management agencies and to reduce casualties<sup>4</sup>. During a catastrophic earthquake, timely mapping of the spatial distribution of ground motion parameters such as peak ground acceleration (PGA), peak ground velocity (PGV), spectrum intensity (SI), and the instrumental JMA (Japan Meteorological Agency) seismic intensity ( $I_{JMA}$ ) in near real-time is crucial to an effective rescue and emergency-response operation. In fact, GIS-based estimation of ground motion values can be used for construction of fragility curves for particular structures where strong motion stations are sparse. Many researchers have identified the correlations between strong ground motion parameters and geology/site classifications<sup>5,6</sup>. Recently, Yamazaki et al.<sup>1</sup> proposed a method to estimate amplification ratios for

strong ground motion parameters that is applicable for all of Japan. They compared the relationship between the geomorphological and geologic conditions of the JMA free-field strong motion stations nationwide and the amplification ratios determined from the attenuation equations based on the JMA strong motion records. The GIS-based DNLI classification was employed to predict unique amplification ratios for PGA, PGV, and  $I_{JMA}$  for a square kilometer mesh that covers all of Japan. In this study, we apply the proposed soil amplification ratios to two recent moderate-magnitude earthquakes in Japan as a practical example in damage assessment for a large area. The results are compared with the results estimated by attenuation models for the both events.

## 2. STRONG MOTION DATA

Two recent earthquakes in Japan, which provided us with reliable data sets, recorded by the strong motion networks of the National Research Institute for Earth Science and Disaster Prevention (NIED) named K-NET<sup>7)</sup> and KiK-net. The October 6, 2000 Tottori earthquake, with JMA magnitude of 7.3 ( $M_W=6.6$ ), depth of 11 km, and left-lateral faulting, occurred in western Japan. The main rupture started 2.5 s after the nucleation and ruptured over a length of 20 km and width of 10 km<sup>8)</sup>. The Geiyo earthquake struck March 24, 2001 ( $M_j=6.7$ ,  $M_w=6.8$ ) when a normal faulting system caused a unilateral rupture that propagated from north to south. The major slip occurred at a depth of 50 km on a fault 25 km long and 10 km wide<sup>9)</sup>. These two events caused slight to moderate damage to structures and lifeline facilities as well as soil liquefaction at the several areas near the coastlines of Hiroshima and western Tottori Prefectures. In order to investigate the ground-motion characteristics and to capture surface variation in ground motion indices we calculated PGA, PGV,  $I_{JMA}$ , and SI from the available strong motion records. Records with a PGA less than  $1 \text{ cm/s}^2$  in one horizontal component were excluded. The shortest distance from each recording station to the fault plane was calculated using the model of Yagi and Kikuchi (2000 and 2001). The final data sets consist of 329 and 454 three-component acceleration records, respectively. Figure 1 demonstrates the variation of PGA with respect to PGV values. The maximum PGA and PGV values in the horizontal component were in excess of  $900 \text{ cm/s}^2$  and  $100 \text{ cm/s}$ , respectively (Figure 1a) and were recorded at station TTRH02 of Hino KiK-net. During the 2001 Geiyo earthquake, the maximum PGA and PGV registered as  $800 \text{ cm/s}^2$  and  $30 \text{ cm/s}$ , respectively at the Yuki K-NET (HRS009) station (Figure 1b).

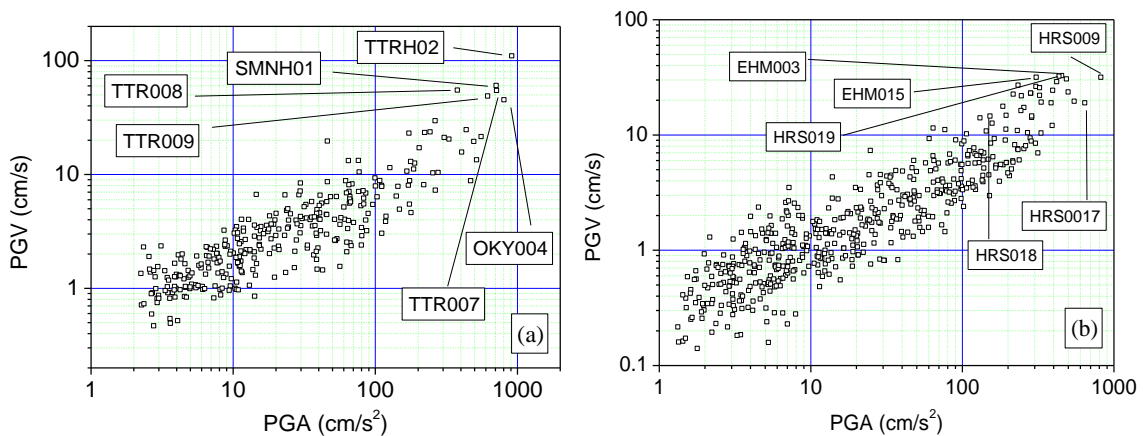


**Figure 1.** Relationship between the observed PGA and PGV for K-NET and KiK-net stations. (a) The 2000 Tottori earthquake and (b) the 2001 Geiyo earthquake.

## 3. SPATIAL DISTRIBUTION OF STRONG MOTION PARAMETERS

The amplification ratios for a  $1 \text{ km} \times 1 \text{ km}$  mesh were calculated following the method proposed by Yamazaki et al.<sup>1)</sup>, that correlates the average station factors of Shabestari and Yamazaki<sup>10)</sup> and the eleven DNLI soil classification groups, which are based on geomorphological and subsurface geology conditions. First, the appropriate DNLI classification was assigned to each recording station and then the strong motion at the ground surface was converted to a base-rock level (outcrop) by applying amplification ratios for the each group.

### 3.1. Attenuation Relationships at the Base Level

There were sufficient numbers of the strong motion records from the two earthquakes to allow construction of attenuation relationship for each event. This eliminated the inter-event component of variability in the attenuation relations. The attenuation model includes near-source saturation effects is given by

$$Y = b_0 + b_1 r + b_2 \log_{10}(r + d) + \varepsilon \quad (1)$$

in which  $Y$  is  $\log_{10}$ PGA,  $\log_{10}$ PGV,  $\log_{10}$ SI, or the  $I_{JMA}$ ,  $r$  is the shortest distance to the fault rupture, the  $b_i$ 's are the regression coefficients to be determined,  $d$  is the near-source saturation effect (in kilometers), and  $\varepsilon$  represents the error term. The terms  $b_1 r$  and  $b_2 \log_{10}(r+d)$  represent anelastic attenuation and geometric spreading, respectively. The coefficient  $b_2$  equals  $-1.89^{(11)}$  for intensity and  $-1.0$  for the PGA, PGV, and SI. The error term is defined as the difference between the predicted ground motion parameters by Eq. (1) for a trial value of  $d$  and the corresponding recorded ground motion indices. The near-source saturation term,  $d$  was applied only to the geometric spreading term. This is because near-source anelastic attenuation is negligible compared with geometric spreading. Since the near-source data from the 2000 Tottori-ken Seibu earthquake used in this study were from a single earthquake, the saturation effect term,  $d$ , was assumed to be constant. An iterative non-linear least square analysis was performed to estimate  $d$ . The error term  $\varepsilon$  was defined as the difference between the predicted ground motion parameters, (Equation 1), for a trial value of  $d$  and the corresponding recorded ground motion values. However, it should be noted that  $d$  was zero for the 2001 Geiyo earthquake since there was no evidence of near-source saturation effects (the shortest distance to the fault extension was more than 40 kilometers).

### 3.2. Stochastic Kriging Method with a Trend Component

Converting the observed values to the hypothetic ground base level minimized the effects of surface layers. Kriging, a stochastic interpolation method, was used to estimate the spatial distributions of strong motion parameters at the base level. First an exponential auto-correlation function was assigned. Simple Kriging algorithm was selected that provided a minimum error-variance estimate of unsampled values from neighboring data low-pass filter allowed smoothing of details and extreme values from the original data set<sup>(12)</sup>. In this study we applied the simple Kriging technique assuming a prior trend component, since the underlying random function model is the sum of a trend and residual components<sup>(13)</sup>:

$$Z(u) = m(u) + R(u) \quad (2)$$

where  $Z(u)$  is the random variable model at location  $u$ ,  $m(u)$  is the trend component, which is modeled as a smoothly varying deterministic function of the coordinates vector  $u$ , and  $R(u)$  is the residual component modeled as a stationary random function with a zero mean and covariance. The trend component (deterministic function) is assigned for the attenuation relation obtained at the base level. The residual component (random function) is defined as the difference between ground motions converted to the base level and the corresponding mean trend component values<sup>(14)</sup>:

$$(u) = X_{bi} - X_{mi} \quad (i = 1, \dots, n) \quad (3)$$

in which  $X$  is  $\log_{10}$ PGA,  $\log_{10}$ PGV,  $\log_{10}$ SI, or  $I_{JMA}$ , and the suffixes  $b$  and  $m$  represent the ground motion value at the base and the mean attenuation value, respectively, for the  $n$  observations. Finally, the spatial distributions of the ground motion parameters at the ground surface are obtained by multiplying the corresponding GIS-based amplification ratio for each pixel.

## 4. RESULTS AND DISCUSSIONS

The spatial distributions of PGA, PGV, SI, and  $I_{JMA}$  for the 2000 Tottori-ken Seibu and the 2001 Geiyo earthquakes, with 79996 and 120376 grid points, respectively, were estimated for the selected regions. Those GIS-based grid points, corresponding to the 1 km  $\times$  1 km pixels of the DNLI, were obtained using the Kriging method described in the previous section. The mapping results of the  $I_{JMA}$  are presented in Figs. 2 and 3. The estimated ground-motion distribution maps look quite natural and match the observed values at the seismic stations. Individually constructing the attenuation relationships and introducing them into the deterministic function (the trend component) of the Kriging method resulted in realistic distributions of the estimated ground motion. The same method was applied to the previous study in

Hyogoken Nanbu (Kobe) earthquake and resulted in a fair correlation between the estimated PGV distribution and the actual damage distribution of highway bridges<sup>14</sup>). In Japan, the JMA developed the nationwide seismic instrumentation and earthquake information broadcasting system. Since 1996, the JMA has deployed over 500 the new JMA-95-type accelerometers throughout Japan<sup>15</sup>). We further examined the accuracy of the Yamazaki et al. (2000) method using acceleration records from the JMA network recorded during the 2000 Tottori and the 2001 Geiyo earthquakes. As in earlier, ground motion values were estimated based on Kriging of the K-NET and KiK-net data and the amplification ratio estimated from the DNLI. The estimated PGA and  $I_{JMA}$  were compared with observed ground motion values recorded by the JMA seismic network stations (Figures 4 and 5). The general trends of the values estimated for the 2000 Tottori earthquake (see circles in Figures 4a and b) are well correlated with the observed JMA ones. The agreement between the observed and estimated values is much worse for the 2001 Geiyo earthquake than for the Tottori earthquake. The dense K-NET and KiK-net stations recorded high frequency radiation from the relatively deep Geiyo earthquake. The amplification ratios employed here for the base-rock conversion may not be adequate for seismic records with rich high-frequency contents. Scatters from the estimations are observed at some stations (see circles in Figures 4 and 5). The current Kriging approach matches the observed values at the observation points used for the interpolation, but between the observation points the estimation approaches the trend component as the distance from the observation points becomes large. Site-specific response characteristics of the JMA stations may be the major cause of the scatters. It is well known that strong motion values are affected by local soil conditions and topography. It may be difficult to reduce the scatter in the data without knowing detailed site response characteristics. Figures 4 and 5 (plus sign) support an inference that the use of an attenuation relation for each earthquake as the trend component in Kriging improves the accuracy of estimated ground motion parameters significantly, compared with the straightforward application of a general attenuation relation. For some earthquakes, like the Geiyo earthquake, a systematic difference from the mean attenuation relation exists. In such cases, the development of an attenuation relation for an individual event reduces the intra-event variability.

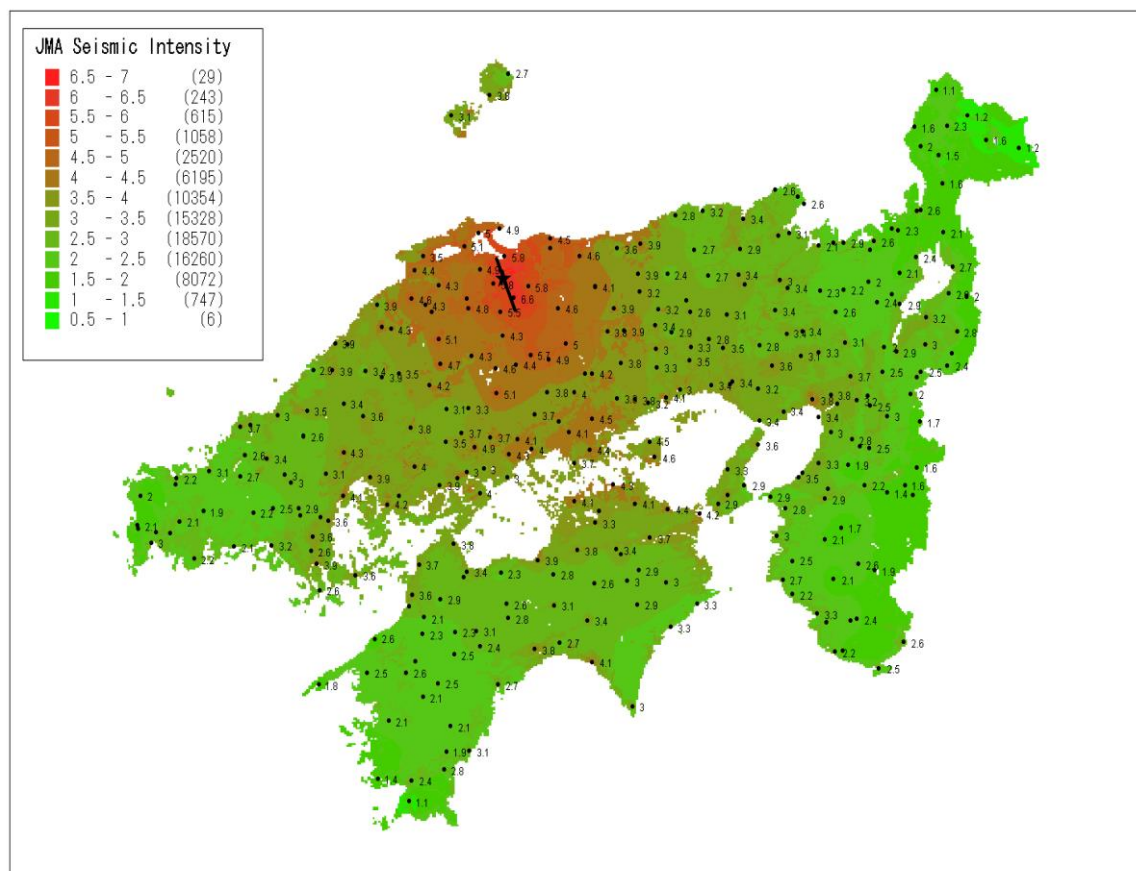


**Figure 2.** GIS-based spatial distribution of the  $I_{JMA}$ , the epicenter (star), and the surface projection (thick line) of the fault plane for the 2000 Tottori earthquake. The result is shown for 1 km  $\times$  1 km pixels of the DNLI. Plotted values are observed ones.

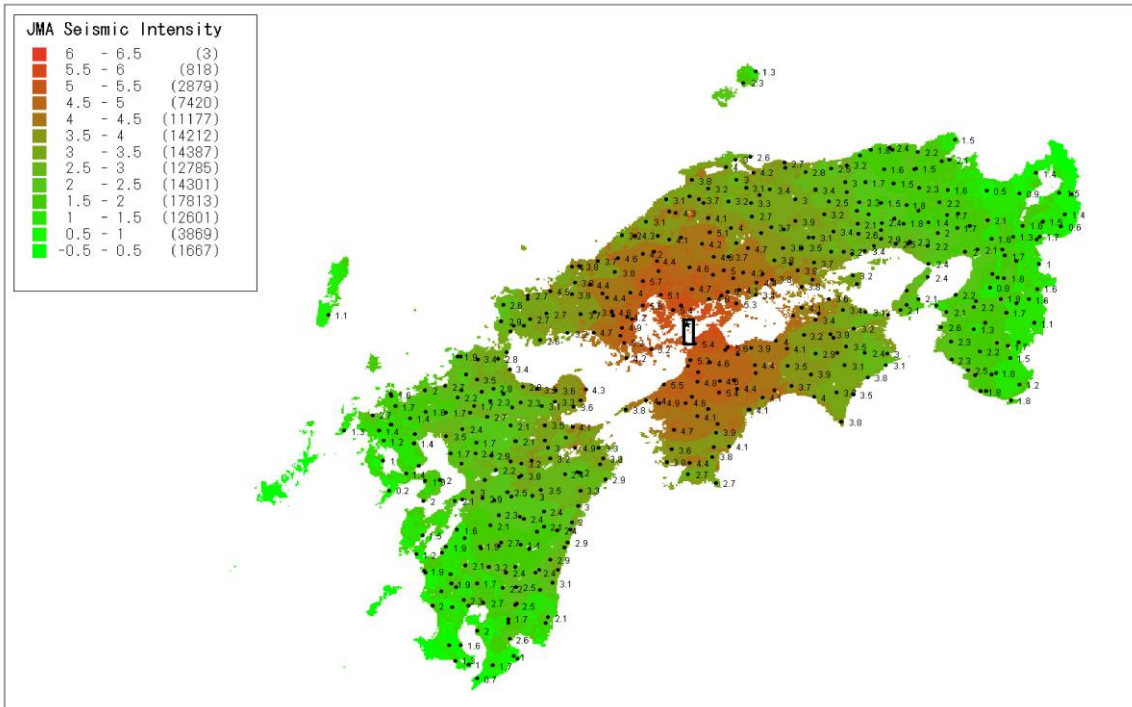


**Figure 3.** GIS-based spatial distribution of the  $I_{JMA}$ , the epicenter (star), and the surface projection (thick line) of the fault plane for the 2001 Geiyo earthquake. The result is shown for  $1 \text{ km} \times 1 \text{ km}$  pixels of the DNLI. Plotted values are observed ones.

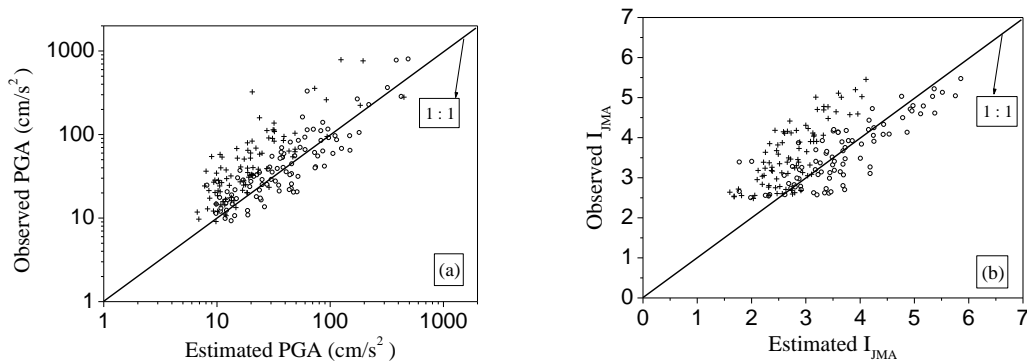


**Figure 4.** Comparison of the observed ground motion recorded by the JMA seismic network and the estimated values in the 2000 Tottori earthquake. The circle shows the strong motion indices at the JMA stations estimated by Kriging using K-NET and KiK-net sites and the amplification ratio from the DNLI. The plus sign indicates the estimated those indices by the empirical attenuation relation of Shabestari and Yamazaki (1998) with the amplification ratio from the DNLI, for (a) the PGA and (b)  $I_{JMA}$ .

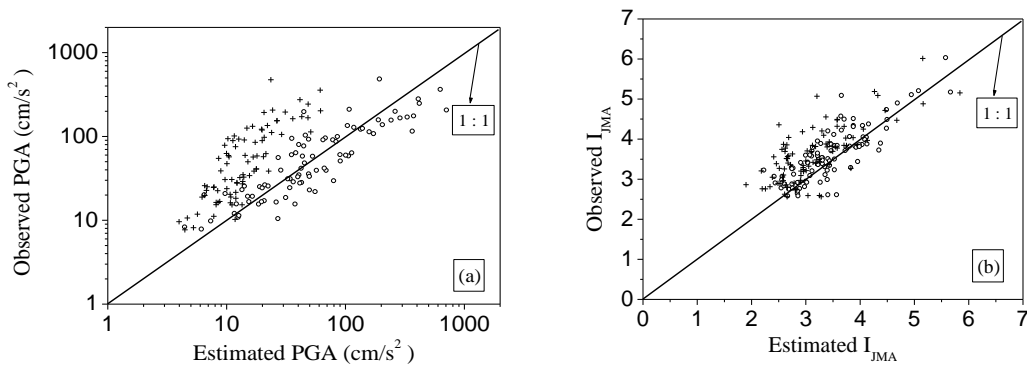


**Figure 5.** Distribution of the observed ground motion parameters by the JMA seismic network and the values estimated for in the 2001 Geiyo earthquake, for (a) PGA and (b)  $I_{JMA}$  (for more details refer to the text).

## 4. CONCLUSIONS

This study was intended to demonstrate the accuracy and applicability of nationwide GIS-based amplification ratios for PGA, PGV, and  $I_{JMA}$ , as recently proposed by Yamazaki et al. (2000) for Japan. We selected strong ground motion records of the 2000 Tottori-ken Seibu and the 2001 Geiyo earthquakes from the K-NET and KiK-net strong motion networks. In order to reduce site amplification effects, we estimated the spatial distribution of strong motion values at base-rock level using a simple Kriging method that introduced an attenuation relationship as a trend component. Multiplying these estimated values by the amplification ratios across 1 km  $\times$  1 km mesh of the DNLI yielded spatial distributions for those parameters at the ground surface. Relatively good correlations between the estimated and recorded ground motion parameters at the JMA seismic stations were observed for both earthquakes. The proposed approach, removed inter-event variability of strong motion indices by introducing an attenuation relation for each event, and intra-event variability was considered as the amplification factor, which was linked with the geologic and topographic conditions in the DNLI. Hence the proposed method can be used to estimate strong motion distributions with reasonable accuracy, leading to early improved earthquake damage assessment in Japan.

## REFERENCES

1. Yamazaki F., K. Wakamatsu, J. Onishi, and K.T. Shabestari (2000). Relationship between geomorphological land classification and soil amplification ratio based on JMA strong motion records, *Journal of Soil Dynamics and Earthquake Engineering*, **19**, 41-53.
2. Kanamori, H., E. Hauksson, and T. Heaton (1997). Real-time seismology and earthquake hazard mitigation, *Nature*, **390**, 461-464.
3. Yamazaki, F., S. Noda, and K. Meguro (1998). Developments of early earthquake damage assessment systems in Japan, *Proc. of 7<sup>th</sup> International Conference on Structural Safety and Reliability*, 1573-1580.
4. Wald, D. J., V. Quitoriano, T.H. Heaton, H. Kanamori, C.W. Scrivner, and C.B. Worden, (1999). TriNet "ShakeMaps": Rapid generation of peak ground motion and intensity maps for earthquakes in southern California, *Earthquake Spectra*, **15**, 3, 537-555.
5. Wills, C.J., M. Petersen, W.A. Bryant, M. Reichle, G.J. Saucedo, S. Tan, G. Taylor, and J. Treiman (2000). A site-conditions map for California based on geology and shear-wave velocity, *Bulletin of the Seismological Society of America*, **90**, 6B, S187-S208.
6. Matsuoka, M. and S. Midorikawa (1995). GIS-based integrated seismic hazard mapping for a large metropolitan area, *Proceedings of the 5th International Conference on Seismic Zonation*, **2**, 1334-1341.
7. Kinoshita, S. (1998). Kyoshin Net (K-NET), *Seismological Research Letters*, **69**, 4, 309-332.
8. Yagi, Y., and M. Kikuchi, (2000). Source rupture process of the October 6, 2000 Tottori-ken Seibu earthquake, <http://wwwweic.eri.u-tokyo.ac.jp/yuji/tottori/>.
9. Yagi, Y., and M. Kikuchi (2001). Source rupture process of the March 24, 2001 Geiyo earthquake, <http://wwwweic.eri.u-tokyo.ac.jp/yuji/Aki-nada/>.
10. Shabestari, T.K., and F. Yamazaki (1998). Attenuation relationship of JMA seismic intensity using JMA records, *Proceedings of the 10th Japan Earthquake Engineering Symposium*, **1**, 529-534.
11. Tong, H., and F. Yamazaki (1996). Relationship between ground motion indices and new JMA seismic intensity, *Seisan-kenkyu*, **48** 11, (in Japanese).
12. Deutsch, C.V., and A.G. Journel (1998). Geostatistical software library and user's guide, Applied Geostatistics Series, The Oxford University Press, New York.
13. Journel, A.G., and M. Rossi (1989). When do we need a trend model in kriging, *Math Geology*, **21**, 7, 715-739.
14. Yamazaki, F., J. Onishi, and S. Tayama (1999). Earthquake damage assessment of expressway structures in Japan, *Proc. of Asian-Pacific Symp. on Structural Reliability and its Applications*, 205-214.
15. Yamazaki, F. (1998). Real-time earthquake disaster mitigation system in Japan, *Seismology and earthquake engineering in Japan*, Property and Casualty Insurance Rating Organization of Japan, 133-149.